

Article

Not peer-reviewed version

In vitro cytotoxic effects of ferruginol analogues in Sk-MEL28 human melanoma cells

[Luying Shao](#)^{*}, [Miguel A. González-Cardenete](#), [Jose M. Prieto-Garcia](#)^{*}

Posted Date: 3 August 2023

doi: 10.20944/preprints202308.0318.v1

Keywords: diterpenes; ferruginol; apoptosis; melanoma; migration, caspases.



Preprints.org is a free multidiscipline platform providing preprint service that is dedicated to making early versions of research outputs permanently available and citable. Preprints posted at Preprints.org appear in Web of Science, Crossref, Google Scholar, Scilit, Europe PMC.

Copyright: This is an open access article distributed under the Creative Commons Attribution License which permits unrestricted use, distribution, and reproduction in any medium, provided the original work is properly cited.

Article

In Vitro Cytotoxic Effects of Ferruginol Analogues in Sk-MEL28 Human Melanoma Cells

Luying Shao ^{1,*}, Miguel A. González-Cardenete ² and Jose M Prieto ^{1,3,*}

¹ School of Pharmacy, University College London, London, UK

² Instituto de Tecnología Química (UPV-CSIC), Universitat Politècnica de Valencia-Consejo Superior de Investigaciones Científicas, Avda de los Naranjos s/n, 46022 Valencia, Spain; migoncar@itq.upv.es

³ Centre for Natural Products Discovery, School of Pharmacy and Biomolecular Sciences, Liverpool John Moores University, Liverpool, United Kingdom; j.m.prietogarcia@ljmu.ac.uk

* Correspondence: luying.shao.12@ucl.ac.uk (L.S.); j.m.prietogarcia@ljmu.ac.uk (J.M.P.)

Abstract: Ferruginol is a promising abietane-type antitumor diterpene able to induce apoptosis in SK-Mel-28 human malignant melanoma. We here aim to increase this activity by testing the effect of a small library of ferruginol analogues. After an screening of their antiproliferative activity (SRB staining) on SK-Mel-28 cells the analogue 18-aminoferruginol (GI₅₀≈10 μM) was further selected for mechanistic studies including effects on mitochondrial viability (MTT assay, IC₅₀≈10 μM *p*<0.0001), induction of apoptosis (DAPI staining, *p*<0.001), changes in cell morphology associated with the treatment (cell shrinkage and membrane blebbing), induction of caspase-3/7 activity (2.5× at 48h, 6.5× at 72h; *p*<0.0001), changes in the mitochondrial membrane potential (not significant), and effects on 2D cell migration and 3D cell invasion (modified Boyden assay, not significant). The results were compared to those of the parent molecule (ferruginol, GI₅₀≈50 μM) and paclitaxel (GI₅₀≈10 nM) as a reference drug. In conclusion, we demonstrate here that derivatization of ferruginol into 18-aminoferruginol increases its antiproliferative activity 5 times in SK-MEL-28 cells as well as changing the apoptotic mechanism of its parent molecule ferruginol from activation of caspases without depolarization of mitochondrial membrane.

Keywords: diterpenes; ferruginol; apoptosis; melanoma; migration; caspases

1. Introduction

Natural products continue to provide lead cytotoxic compounds for cancer treatment [1]. Malignant melanoma is the most aggressive form of skin cancer and accounts for about 3% of all cases of malignant tumour. Its incidence is increasing worldwide, and it is becoming resistant to current therapeutic agents [2].

We recently reviewed the therapeutical potential of diterpenes against melanoma [3]. This phytochemical class presents a high structural diversity some with potent biological activities due to their unique carbon skeletons. They been a classic source for the development of new anticancer agents, the first “blockbuster diterpene” being Taxol, which was originally selected due to its activity on murine melanoma cells [4]. The latest discovery in this class of metabolites is ingenol mebutate which is indicated for the chemoprevention of melanoma in actinic keratosis patients [3].

Abietane-type diterpenes are characterized by a tricyclic ring system. Some of them have been identified as active cytotoxic principles against melanoma cells. These include carnosol and carnosic acid, two well-known phenolic diterpenes from *Rosmarinus officinalis* L. (Lamiaceae) extracts [5,6] as well as other lesser known diterpenes such as Parvifloron D, a natural diterpene isolated from *Plectranthus ecklonii* Benth [7], 11,12,16-trihydroxy-2-oxo-5-methyl-10-demethyl-abieta-1[10],6,8,11,13-pentene isolated from *Premna serratifolia* L. [8], and 7a-acetoxyroyleanone and horminone from roots of *Peltodon longipes* A. St. Hill. Ex Benth [9]. All these plants belong to the same botanical family (Lamiaceae). Another abundant source of these diterpenes is the rosin from coniferous species such as pine trees. Abietic acid and dehydroabietic acid, which are the main diterpenic resin acids found in *Pinus* rosin, have been found to have potential as anticancer agents.

They have shown strong growth inhibitory activity against various human cancer cell lines, including those of the breast, ovary, prostate, colon, liver, lung, and cervix [10].

Ferruginol (**1**, Figure 1) is another promising abietane-type antitumor diterpene with a characteristic phenolic ring, found in the Lamiaceae and Cupressaceae families [11]. It significantly exerted various cytotoxic effects on gastric, prostate, lung, cervical, breast and colon cancer cells, together with leukemia and melanoma cells in vitro [12], as well as tumour growth in mice CL1-5 xenografts when administered via *i.p.* [13]. Sugiol, the C7-oxidized ferruginol derivative (**11**, Figure 1) has also shown in vitro cytotoxic activity against human pancreatic and melanoma tumor cell models [12] and in vivo antitumor properties in a prostate DU145 mouse xenograft model [14].

Ferruginol is also known to induce apoptosis on SK-Mel-28 human malignant melanoma cells mediated through P-p38 and NF- κ B [15]. Following on this data, we here aim to further our knowledge on the effect of a small library of ferruginol analogues (Figure 1) in human SK-MEL-28 melanoma cells. The test compounds in this study are depicted in Figure 1.

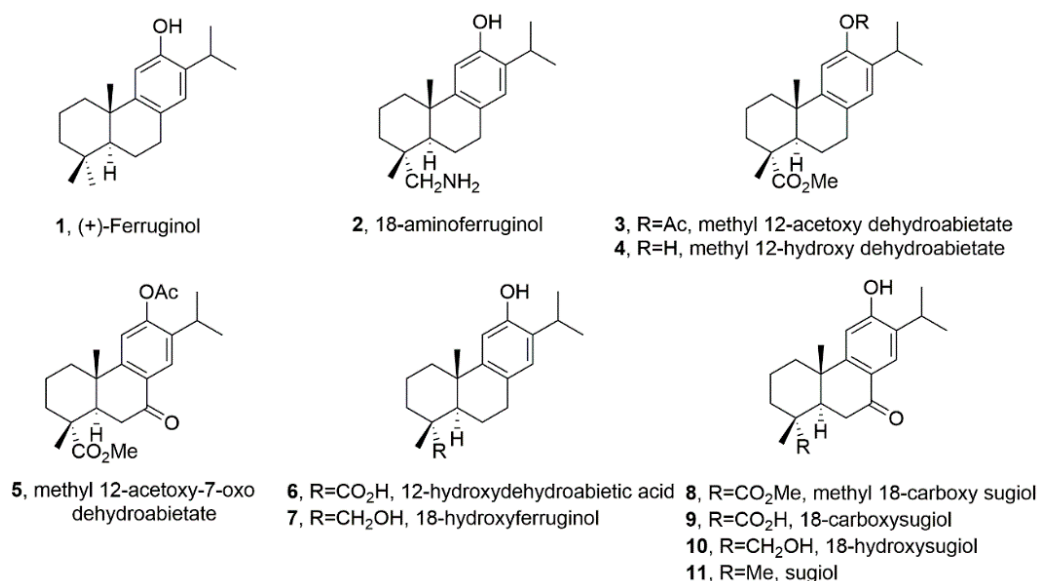


Figure 1. Chemical structures of ferruginol and analogues studied in this work.

2. Results

2.1. Antiproliferative activity of ferruginol and analogues

Figure 2 shows the (GI₅₀) in the SRB assay (48h, μ M) of tested ferruginol analogues in SK-MEL-28 cells. Paclitaxel (GI₅₀ = 10 nM) was used as a positive reference (not shown in the figure).

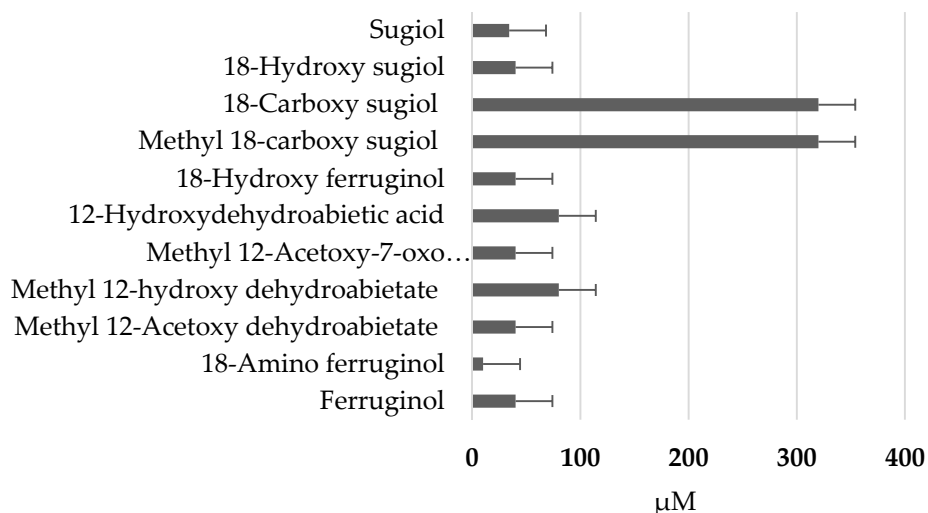


Figure 2. Antiproliferative activity (GI₅₀, μM) in the SRB assay (48h) of ferruginol analogues in SK-MEL-28 cells.

The cytotoxic activity of ferruginol and 18-aminoferruginol (compound 2) resulted 47.5 and 9.8 μM, respectively. Figure 3 shows the dose-activity relationship for these two compounds.

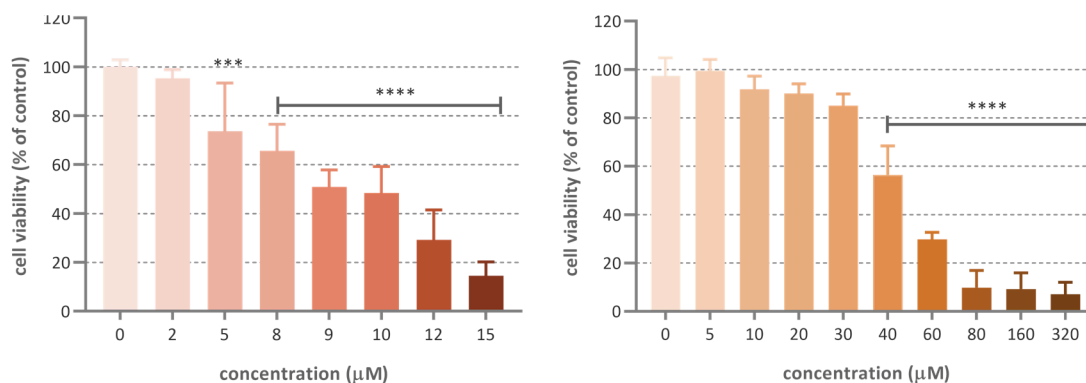


Figure 3. SK-MEL-28 proliferation after treatment with 18-aminoferruginol (left bar graph) and ferruginol (right bar graph) (SRB assay, 48h, μM). Mean ± SD (n=4), (***) $p < 0.001$; (****) $p < 0.0001$.

2.3. Induction of apoptosis and changes in cell morphology associated with the treatment

A qualitative evaluation of cell viability and apoptosis was conducted using phase contrast microscopy and DAPI staining to confirm that compounds were cytotoxic to melanoma cells and to reflect the findings of the SRB assay. The percentage of blue-stained cells after exposure treatments for 48h were elevated compared to the control, indicating that both compounds promoted cell death (Figure 4, right column). Also, phase contrast images (Figure 4, left column) show that untreated cells grew to near confluence and were able to spread regularly in the slide, whereas cells treated displayed several apoptotic features such as cell shrinkage and membrane blebbing over the incubation period. Quantitative evaluation of the images was performed in terms of count of the total number of nuclei normalized to untreated controls and total number of fragmented nuclei (Figure 5).

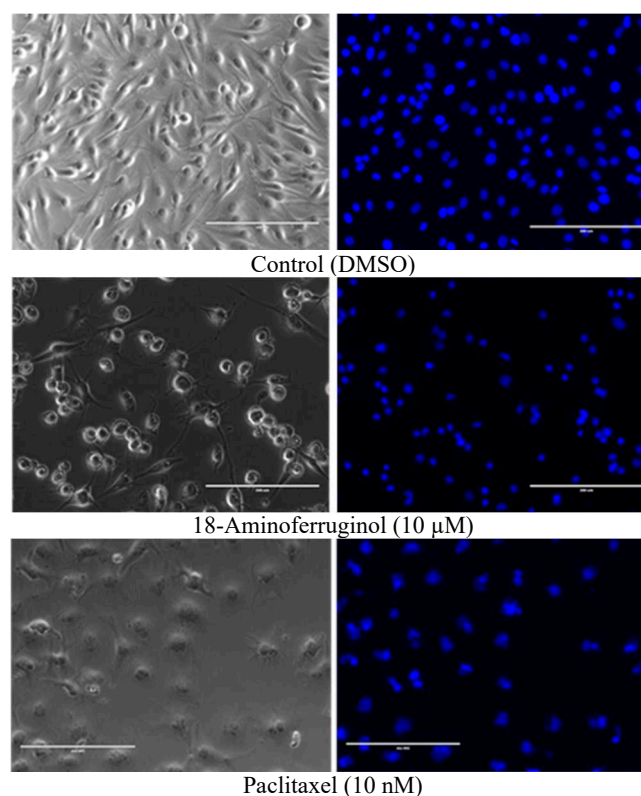


Figure 4. Representative light contrast microscopy (left) and fluorescence DAPI (right) 20× images of living SK-MEL-28 cells after treatment with 18-Aminoferruginol (48h). Paclitaxel is used as positive reference (48h).

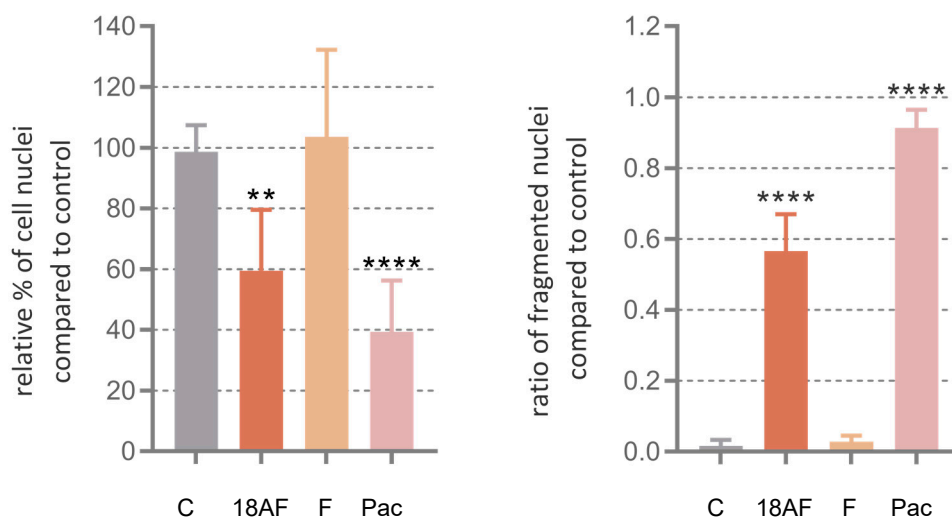


Figure 5. Quantification of DAPI staining. On the left, count of the total number of nuclei normalized to untreated controls (C) (average of 3 fields per condition from 3 separate plates; $n=9$ fields per condition); On the right, count of a total number of fragmented nuclei over the total number of nuclei (average of 3 fields per condition from 3 separate plates; $n=9$ fields per conditions). Mean and standard errors are shown. P-values were calculated by one-way ANOVA followed by Dunnet's test, $P^{**}<0.01$ and $P^{****}<0.0001$. Paclitaxel (Pac) was used as positive control.

2.4. Induction of caspase-3/7 activity

Caspase-3/7 activity was induced upon cell exposure to the compounds with time-dependent enhancement in the treated cells. Only 18-aminoferruginol (10 μ M) promoted caspase-3/7 activity in a comparable manner to the reference drug paclitaxel (10 nM) at all times. (Figure 6).

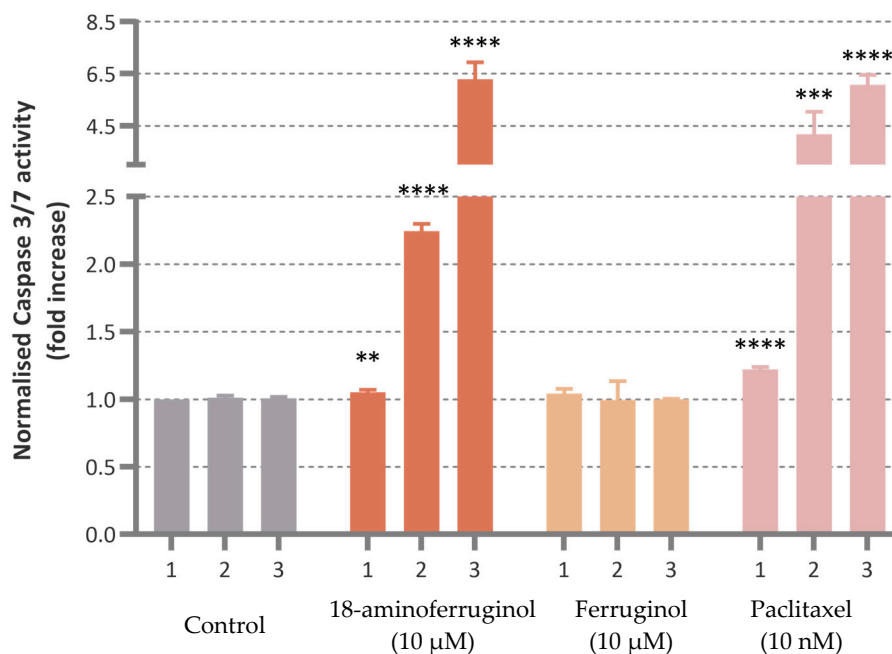


Figure 6. The effect of ferruginol (10 μ M) and compound 2(10 μ M) on caspase-3/7 activity of in SK-MEL-28 cells (12, 24 and 48h). Results are Mean \pm SD (n=4), p-value were determined via one-way ANOVA followed by Dunnet's test, (**) $p < 0.01$; (***) $p < 0.001$; (****) $p < 0.0001$. Paclitaxel (Pac) was used as positive control.

2.5. Mitochondrial membrane potential

Although ferruginol (10 μ M) was able to depolarize mitochondrial membranes in a comparable manner as the reference compound CCCP, its cytotoxic derivative 18-aminoferruginol (10 μ M) failed to do so.

2.6. 2D Migration assay and 3D Invasion assay

Both ferruginol and its derivative compound 2 (18-aminoferruginol) failed to either inhibit migration or invasion at 10 μ M (Data not shown).

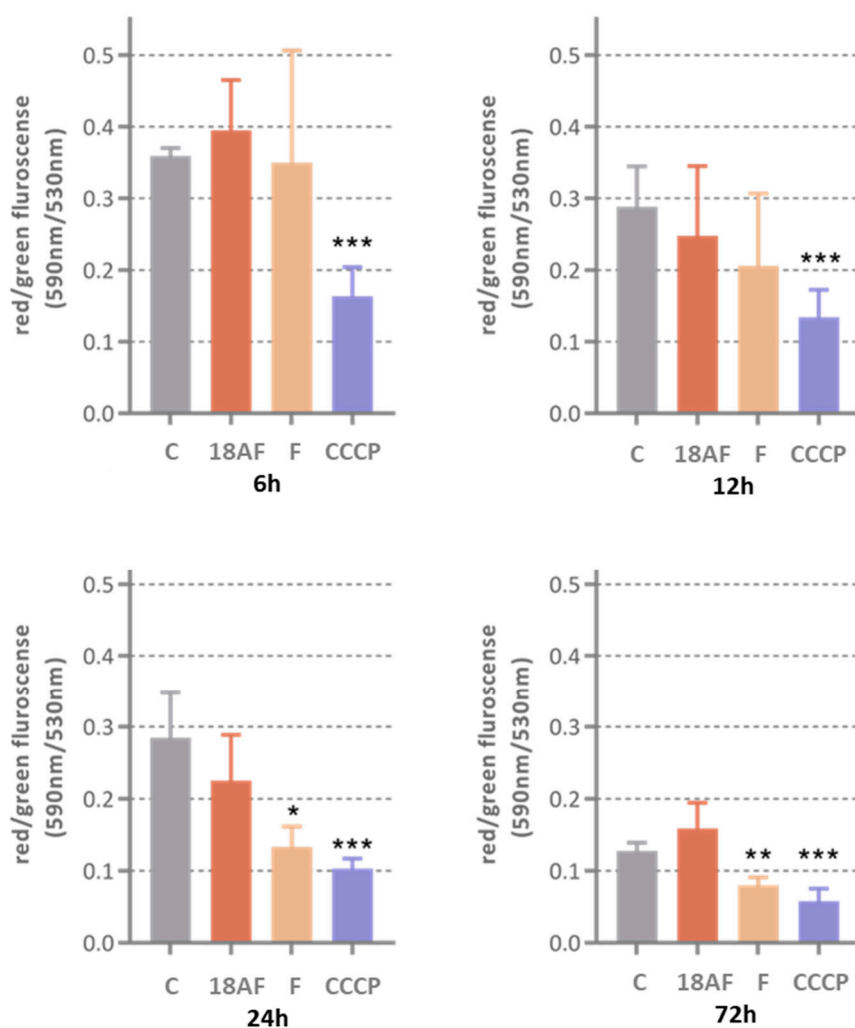


Figure 7. The effect of ferruginol (10 and compound 2 on mitochondrial membrane potential (10 μ M) at various treatment times (6h, 12h, 24h and 72h). Results are Mean \pm SD (n=4), p-value were determined via one-way ANOVA followed by Dunnet's test, (*) $p < 0.05$; (**) $p < 0.01$; (***) $p < 0.001$. CCCP was used as positive control.

3. Discussion

Ferruginol has been described as inducing apoptosis in several melanoma cell lines including SK-MEL-28 [12,15]. In our case, it marginally failed to significantly do so at 12h treatment in SK-MEL-28 melanoma cells, at later timepoints only its 18-amino derivative consistently keeps the antiapoptotic effect by inhibition of these enzymes. Conversely, 18-aminoferruginol fails to reproduce the depolarizing effect of its parent molecule.

Basic structure-activity relationship (SAR) of compounds **1-11** (Figure 1) can be deduced from the obtained data in the SK-MEL-28 cell line (Figure 2). For example, it can be said that most of the compounds were less active and only compounds **1**, **2** and **5** presented a moderate activity being the most potent compound **2** (18-aminoferruginol). Apparently, acetylation on the hydroxyl group at C-12 results in more potent compounds (compounds **3** and **5** vs **4** and **8**). On the contrary, oxygenation at C-7 to give ketone analogues of sugiol **11**, together with methyl ester or carboxylic acid at C-18 such as compounds **8** and **9** led to inactive compounds. The same trend was also found in our previous study with leukemia cell lines [16].

It is noteworthy the amino group at C-18, compound **2**, resulting in an enhanced activity of the parent ferruginol **1**. This is in agreement with previous studies departing from slightly different parent abietane templates. Dehydroabietylamine -also called leelamine- have been shown to be a better antitumour agent when compared to its parent molecule dehydroabietic acid [17]. It targets

multiple key signaling pathways in melanoma cells [18], including uncommon ones such cancer cell death through inhibition of intracellular cholesterol transport [19]. This prompted the synthesis of further derivatives -such as abietylamine- to try and improve on these bioactivities [16,20] as well as protecting intellectual property [21]. A major difference of these derivatives with ferruginol is the absence of the phenol group.

In summary, we demonstrate here that derivatization of ferruginol into 18-aminoferruginol increases its antiproliferative activity 5 times in SK-MEL-28 cells as well as changing the apoptotic mechanism from activation of caspase without depolarization of the mitochondrial membrane.

4. Materials and Methods

4.1. Materials

Ferruginol and synthetic analogues (Figure 1) were synthesized as described previously by Gonzalez Cardenete [16,20], all other chemicals were purchased from Sigma-Aldrich (St. Louis, MO, USA) Sulforhodamine B, trichloroacetic acid, Trizma base, propidium iodide, Ribonuclease A, formaldehyde and crystal violet. Glacial acetic acid, ethanol and methanol were obtained from Fisher (Leicestershire, UK). Minimum essential media (MEM), heat-inactivated fetal bovine serum (FBS), penicillin-streptomycin antibiotic, non-essential amino acids solution (NEEA), sodium pyruvate, TrypLE Express (1×, trypsin, EDTA, phenol red), phosphate-buffered saline (PBS), ReadyProbes® cell viability imaging kit trypan blue, MitoProbe JC-1 kit were purchased from Thermo Fisher Scientific (Waltham, MA, USA). Matrigel was purchased from BD Bioscience (San Jose, CA, USA), Caspase-Glo® 3/7 from Promega, DAPI staining from Cell Signalling Technology (Danvers, MA, USA). CytoSelect Cell Migration Assay kit were from Cell Biolab Inc.

4.2. Cell lines

SK-MEL-28 cell line was purchased from American Type Culture Collection (Manassas, VA, USA) and were maintained in MEM containing GlutaMAX and supplemented with 10% FBS, 1% NEEA, 1mM sodium pyruvate and 1% penicillin-streptomycin antibiotic under a humidified atmosphere (Air 5% CO₂) and at 37°C.

4.3. Sulforhodamine B (SRB) assay

This assay determined the ability of the extract to inhibit cellular growth by measuring the cell density, thereby estimate cell number. This assay was performed according to previously described methods [22]. Cells were seeded at density of 8,000 cells/well in a 96-well plate (Thermo Scientific) and left overnight to attach at 37°C. Afterwards, cells were treated with ferruginol and its derivatives for 48h. Upon the completion of the incubation period, the cells were fixed with trichloroacetic acid solution for one hour at 4°C. After washing with water, cellular protein was stained with SRB solution and left at room temperature for one hour. followed by washing the plate four times with 1% acetic acid and flicked to remove unbound dye. Then, Tris base buffer solution was added to each well and the absorbance was measured at 510 nm. Cell growth was calculated using the following equation:

$$\% \text{Cell growth} = \frac{(\text{Absorbance (sample)} - \text{Absorbance (blank)})}{(\text{Absorbance (vehicle control)} - \text{Absorbance (blank)})} \times 100$$

4.4. Caspase-3/7 activity assay

The apoptosis induced by compounds was determined by measuring the activity of caspase-3/7 using Caspase-Glo® 3/7 according to the manufacturer's protocol (Promega, Madison, WI, USA). SK-MEL-28 cells were seeded in a 96-well white plate and treated with compounds or DMSO for different time points (12, 24 and 48h). Afterwards, 100 µL of culture media of each well was transferred to a 96 white multi-well plate and 100 µL of Caspase-Glo® 3/7 reagent was added and incubated for 1h at room temperature. When the incubation period was completed, the luminescence of each sample

representing the enzymatic activity of caspase was measured using a plate-reading luminometer (Tecan, Switzerland). The assay was performed in three independent experiments and each sample was performed in triplicate (mean \pm SD, n=9).

4.5. Phase-contrast and fluorescence microscopy DAPI staining

Morphological assessment of the cells was performed to detect the cellular changes induced by the tested compounds according to a previously reported method [5]. Cells were seeded at a density of 5000 cells in 12 well plates with or without compounds/DMSO for 48h. Treated cells with typical morphological changes of apoptosis were imaged using a phase-contrast inverted microscope (EVOS cell imaging system, Thermo Fisher Scientific, Waltham, MA, USA).

Cells were treated in the same condition and examined with a fluorescence microscope using DAPI staining dye (Cell signaling Technology, Danvers, MA, USA). The dyes were added and incubated at 37°C for 15 mins and the wells were visualised using the EVOS cell imaging system. The results were obtained by capturing images for six random fields for each sample from three different experiments.

4.6. Determination of Mitochondrial Membrane Potential (MMP)

The mitochondrial transmembrane potential ($\Delta\psi_m$) induced by the compounds in the cancer cell line was determined by using the appropriate fluorescent probe known as JC-1 (Thermo Fisher Scientific, Waltham, MA, USA). 1000 cells/well (for 6,12 and 24h) and 5000 cells/well (for 72h) was seeded into 96 well black-transparent bottoms well plate and incubated. After incubation, the treated cells were washed with the warm phosphate-buffered saline (PBS) twice, JC-1 dye and CCCP (positive control) were added and further incubated for 15 mins at 37 °C in a 5% CO₂ atmosphere. The fluorescence stained cells were measured by fluorescence plate reader (Tecan Infinite M200) with red fluorescence in excitation (550nm)/emission (600nm) and green fluorescence in excitation (485nm)/emission(535nm).

4.7. 2D Migration assay

Cell migration was measured using the CytoSelect Cell Migration Assay kit (CBA-100-C, Cell Biolab Inc.). Polycarbonate filters with an 8- μ m pore size inserts were placed in a 24-well plate. SK-MEL28 cells were seeded in serum-free medium with testing drug onto the inserts and the lower chambers were filled with same serum medium containing drugs and incubated for 24h and 48h. Later, the remaining cells were gently removed using a cotton swab and the inserts were washed and fixed with cold methanol. Then, the migrated cells were stained with 0.5% crystal violet for 10 mins, then inserts were washed with PBS and left air dry. Air-dried inserts were dissolved in 10% acetic acid to obtain colored solution. The number of the cells that migrated to the lower side of the filter was measured at 560nm by using a microtiter plate reader (Tecan Infinite[®] M200) and presented as relative absorbance compared to control (mean \pm SD) from three independent experiments.

4.8. 3D Invasion assay

Cell invasion was measured using the CytoSelect Cell Migration Assay kit (CBA-100-C, Cell Biolab Inc.). Polycarbonate filters with an 8- μ m pore size inserts coated with a protein matrix isolated from Engelbreth-Holm-Swarm tumour cells to form a membrane layer. The coated inserts required rehydration with 300 μ l warm, serum-free medium before cell seeding. SK-MEL28 cells were seeded in serum-free medium with testing drug onto the inserts and the lower chambers were filled with same serum medium containing drugs and incubated for 24h and 48h. Later, the remaining cells were gently removed using a cotton swab and the inserts were washed and fixed with cold methanol. Then, the migrated cells were stained with 0.5% crystal violet for 10 mins, then inserts were washed with PBS and left air dry. Air-dried inserts were dissolved in 10% acetic acid to obtain colored solution. The number of the cells that migrated to the lower side of the filter was measured at 560nm

by using a microtiter plate reader (Tecan Infinite® M200) and presented as relative absorbance compared to control (mean \pm SD) from three independent experiments.

4.9. Statistical analysis

Results are expressed as mean \pm standard deviation (SD) from at least three independent experiments. All data were analysed using One way ANOVA and using unpaired two-tailed Student's t-test with a *p*-value of <0.05 considered as significant to find the statistical significance between treated groups and controls using InStat v.3 (GraphPad, San Diego, USA).

Author Contributions: Conceptualization, Miguel González-Cardenete and Jose Prieto-Garcia; Formal analysis, Luying Shao; Investigation, Luying Shao; Methodology, Luying Shao and Jose Prieto-Garcia; Resources, Miguel González-Cardenete; Supervision, Jose Prieto-Garcia; Writing – original draft, Jose Prieto-Garcia; Writing – review & editing, Luying Shao, Miguel González-Cardenete and Jose Prieto-Garcia.

Funding: This research received no external funding.

Data Availability Statement: The data presented in this study are available on request from the correspondent author. The data are not publicly available until the publication of the first author's PhD dissertation.

Acknowledgements: We would like to thank Dept Pharmaceutics for allowing some lab experiments to be conducted in his cell lab at School of Pharmacy, UCL.

Conflicts of Interest: The authors declare no conflict of interest.

Sample Availability: Samples of the compounds are available from M.A.G.C.

References

1. Newman, D.J.; Cragg, G.M. Natural Products as Sources of New Drugs over the Nearly Four Decades from 01/1981 to 09/2019. *J Nat Prod* **2020**, *83*, 770-803, doi:10.1021/acs.jnatprod.9b01285.
2. Winder, M.; Virós, A. Mechanisms of Drug Resistance in Melanoma. *Handb Exp Pharmacol* **2018**, *249*, 91-108, doi:10.1007/164_2017_17.
3. Prieto, J.M.; Silveira, D. Natural Cytotoxic Diterpenoids, a Potential Source of Drug Leads for Melanoma Therapy. *Curr Pharm Des* **2018**, *24*, 4237-4250, doi:10.2174/1381612825666190111143648.
4. Wall, M.E.; Wani, M.C. Camptothecin and Taxol: Discovery to Clinic—Thirteenth Bruce F. Cain Memorial Award Lecture1. *Cancer Research* **1995**, *55*, 753-760.
5. Cattaneo, L.; Cicconi, R.; Mignogna, G.; Giorgi, A.; Mattei, M.; Graziani, G.; Ferracane, R.; Grosso, A.; Aducci, P.; Schininà, M.E.; et al. Anti-Proliferative Effect of Rosmarinus officinalis L. Extract on Human Melanoma A375 Cells. *PLoS One* **2015**, *10*, e0132439, doi:10.1371/journal.pone.0132439.
6. Alcaraz, M.; Achel, D.G.; Olivares, A.; Olmos, E.; Alcaraz-Saura, M.; Castillo, J. Carnosol, radiation and melanoma: a translational possibility. *Clin Transl Oncol* **2013**, *15*, 712-719, doi:10.1007/s12094-012-0994-9.
7. Silva, C.O.; Molpeceres, J.; Batanero, B.; Fernandes, A.S.; Saraiva, N.; Costa, J.G.; Rijo, P.; Figueiredo, I.V.; Faísca, P.; Reis, C.P. Functionalized diterpene parvifloron D-loaded hybrid nanoparticles for targeted delivery in melanoma therapy. *Ther Deliv* **2016**, *7*, 521-544, doi:10.4155/tde-2016-0027.
8. Habtemariam, S.; Varghese, G.K. A novel diterpene skeleton: identification of a highly aromatic, cytotoxic and antioxidant 5-methyl-10-demethyl-abietane-type diterpene from *Premna serratifolia*. *Phytother Res* **2015**, *29*, 80-85, doi:10.1002/ptr.5229.
9. Fronza, M.; Murillo, R.; Ślusarczyk, S.; Adams, M.; Hamburger, M.; Heinzmann, B.; Laufer, S.; Merfort, I. In vitro cytotoxic activity of abietane diterpenes from *Peltodon longipes* as well as *Salvia miltiorrhiza* and *Salvia sahendica*. *Bioorg Med Chem* **2011**, *19*, 4876-4881, doi:10.1016/j.bmc.2011.06.067.
10. Faustino, C.; Neto, Í.; Fonte, P.; Macedo, A. Cytotoxicity and Chemotherapeutic Potential of Natural Rosin Abietane Diterpenoids and their Synthetic Derivatives. *Curr Pharm Des* **2018**, *24*, 4362-4375, doi:10.2174/1381612825666190112162817.
11. González, M.A. Aromatic abietane diterpenoids: their biological activity and synthesis. *Nat Prod Rep* **2015**, *32*, 684-704, doi:10.1039/c4np00110a.
12. Chan, E.W.C.; Wong, S.K.; Chan, H.T. Ferruginol and Sugiol: A Short Review of their Chemistry, Sources, Contents, Pharmacological Properties and Patents. *Tropical Journal of Natural Product Research (TJNPR)* **2023**, *7*, 2325-2336, doi:http://www.doi.org/10.26538/tjnpr/v7i2.4.

13. Ho, S.T.; Tung, Y.T.; Kuo, Y.H.; Lin, C.C.; Wu, J.H. Ferruginol inhibits non-small cell lung cancer growth by inducing caspase-associated apoptosis. *Integr Cancer Ther* **2015**, *14*, 86-97, doi:10.1177/1534735414555806.
14. Jung, S.N.; Shin, D.S.; Kim, H.N.; Jeon, Y.J.; Yun, J.; Lee, Y.J.; Kang, J.S.; Han, D.C.; Kwon, B.M. Sugirol inhibits STAT3 activity via regulation of transketolase and ROS-mediated ERK activation in DU145 prostate carcinoma cells. *Biochem Pharmacol* **2015**, *97*, 38-50, doi:10.1016/j.bcp.2015.06.033.
15. Jia, Y.; Wu, C.; Zhang, B.; Zhang, Y.; Li, J. Ferruginol induced apoptosis on SK-Mel-28 human malignant melanoma cells mediated through P-p38 and NF- κ B. *Human & Experimental Toxicology* **2019**, *38*, 227-238, doi:10.1177/0960327118792050.
16. Hamulić, D.; Stadler, M.; Hering, S.; Padrón, J.M.; Bassett, R.; Rivas, F.; Loza-Mejía, M.A.; Dea-Ayuela, M.A.; González-Cardenete, M.A. Synthesis and Biological Studies of (+)-Liquiditerpenoic Acid A (Abietopinoic Acid) and Representative Analogues: SAR Studies. *Journal of Natural Products* **2019**, *82*, 823-831, doi:10.1021/acs.jnatprod.8b00884.
17. Gowda, R.; Inamdar, G.S.; Kuzu, O.; Dinavahi, S.S.; Krzeminski, J.; Battu, M.B.; Voleti, S.R.; Amin, S.; Robertson, G.P. Identifying the structure-activity relationship of leelamine necessary for inhibiting intracellular cholesterol transport. *Oncotarget* **2017**, *8*, 28260-28277, doi:10.18632/oncotarget.16002.
18. Gowda, R.; Madhunapantula, S.V.; Kuzu, O.F.; Sharma, A.; Robertson, G.P. Targeting multiple key signaling pathways in melanoma using leelamine. *Molecular cancer therapeutics* **2014**, *13*, 1679-1689, doi:10.1158/1535-7163.Mct-13-0867.
19. Kuzu, O.F.; Gowda, R.; Sharma, A.; Robertson, G.P. Leelamine mediates cancer cell death through inhibition of intracellular cholesterol transport. *Molecular cancer therapeutics* **2014**, *13*, 1690-1703, doi:10.1158/1535-7163.Mct-13-0868.
20. González, M.A.; Pérez-Guaita, D. Short syntheses of (+)-ferruginol from (+)-dehydroabietylamine. *Tetrahedron* **2012**, *68*, 9612-9615, doi:https://doi.org/10.1016/j.tet.2012.09.055.
21. Robertson, G.P.; Raghavendragowda, C.D.; Madhunapantula, S.V.; Kuzu, O.F.; Inamdar, G.S. Compositions and methods relating to proliferative diseases. 2017.
22. Skehan, P.; Storeng, R.; Scudiero, D.; Monks, A.; McMahon, J.; Vistica, D.; Warren, J.T.; Bokesch, H.; Kenney, S.; Boyd, M.R. New colorimetric cytotoxicity assay for anticancer-drug screening. *J Natl Cancer Inst* **1990**, *82*, 1107-1112, doi:10.1093/jnci/82.13.1107.

Disclaimer/Publisher's Note: The statements, opinions and data contained in all publications are solely those of the individual author(s) and contributor(s) and not of MDPI and/or the editor(s). MDPI and/or the editor(s) disclaim responsibility for any injury to people or property resulting from any ideas, methods, instructions or products referred to in the content.